

RESEARCH

Open Access



Evaluation of the influenza vaccine protection in the house dust mite-induced chronic allergic asthma mice model and the evaluation of squalene oil in water emulsion as an adjuvant candidate

So Yeon Ahn¹, Thi Len Ho² and Eun-Ju Ko^{1,2,3*}

Abstract

Background Despite the importance of influenza vaccination in asthma patients, the efficacy of this vaccine in asthma has not been well elucidated. We aimed to compare the efficacy of an influenza vaccine of the asthmatic and control mice. We also evaluated the efficacy of AddaVax™ as an adjuvant candidate, which is equivalent to the MF59 influenza vaccine adjuvant in the elderly.

Method House dust mite extracts were intranasally injected into six-week-old female BALB/c mice to induce chronic allergic asthma. Antibody responses after split-inactivated A/Puerto Rico/8/34 H1N1 influenza vaccination with or without AddaVax™ adjuvant were measured using ELISA. Homologous viral protection was determined by measuring the survival rate, lung inflammation level, and lung virus titer after challenge with the human influenza virus strain A/Puerto Rico/8/1934 H1N1. Antigen-specific T cell responses were determined using flow cytometry.

Result The chronic asthma mice immunized with split-inactivated A/Puerto Rico/8/34 H1N1 influenza vaccine showed significant weight loss and higher lung viral load after homologous influenza infection than naïve vaccinated mice. Antigen-specific IgG, IgG1, and IgG2a production did not differ between the naïve and asthma mice. However, serum HI titer was lower in asthma-vaccinated mice after infection. The application of AddaVax™ to a vaccine for mice with asthma enhanced the efficacy of homologous antiviral protection but elicited eosinophil infiltration in the lungs after homologous influenza virus infection.

Conclusion The immune response after split inactivated A/PR8 vaccine differed between asthma and naïve mice, particularly in terms of antibody activity and T cell populations. This study enhances our understanding of how asthma status may influence the effectiveness of influenza vaccine and offers insights into the AddaVax™-induced eosinophilic inflammation, guiding the development of virus vaccine strategies for both healthy individuals and asthma patients.

Keywords Influenza vaccine, Asthma, HDM-induced asthma, AddaVax™, Adjuvant, T cell

*Correspondence:

Eun-Ju Ko

eunju@jejunu.ac.kr

Full list of author information is available at the end of the article



© The Author(s) 2025. **Open Access** This article is licensed under a Creative Commons Attribution-NonCommercial-NoDerivatives 4.0 International License, which permits any non-commercial use, sharing, distribution and reproduction in any medium or format, as long as you give appropriate credit to the original author(s) and the source, provide a link to the Creative Commons licence, and indicate if you modified the licensed material. You do not have permission under this licence to share adapted material derived from this article or parts of it. The images or other third party material in this article are included in the article's Creative Commons licence, unless indicated otherwise in a credit line to the material. If material is not included in the article's Creative Commons licence and your intended use is not permitted by statutory regulation or exceeds the permitted use, you will need to obtain permission directly from the copyright holder. To view a copy of this licence, visit <http://creativecommons.org/licenses/by-nc-nd/4.0/>.

Background

Asthma is a chronic airway inflammatory disease that affects 300 million people worldwide [1]. They have altered immune status and structural remodeling in the airway due to allergen-induced chronic inflammation [2, 3]. Malfunction of the airway and exacerbation of asthma increase the risk of developing severe complications of influenza virus infection. During the 2009 influenza A H1N1 pandemic (pH1N1), asthma was one of the most common underlying medical conditions among patients hospitalized for pH1N1 infections in the U.S. and worldwide [4]. However, despite the importance of influenza vaccination in patients with asthma, there has been limited research on the effectiveness of vaccines and the detailed T cell function against viral infection in asthma.

Allergic asthma is the most common type of asthma [5]. It exhibits pathological features of airway remodeling, including airway thickening, narrowing, edema, and mucous plugging [6, 7]. It is immunologically characterized by allergen-specific immunoglobulin E (IgE) production and eosinophil-dominant T-helper type 2 (Th2)-biased inflammation [8–10]. In a previous study, we demonstrated an increased percentage of exhausted T cells after chronic allergen exposure, with decreased influenza virus clearance in an asthma mouse model [11]. T cell exhaustion refers to the gradual regression of T cell function and number owing to the persistence of low-grade chronic inflammation [12, 13]. These findings suggest that asthma can cause immune dysfunction owing to prolonged inflammation, which may raise concerns about the reduced response to vaccination.

Influenza virus is a highly mutable ssRNA virus, with new strains emerging every year. The success of annual influenza vaccine protection is highly dependent on the accuracy of the prediction of prevalent viruses during the upcoming flu season [14]. Therefore, a robust and effective vaccine that covers both homologous and heterologous strains is needed to reliably increase the success rate of influenza vaccines, which is even more important for people with asthma.

In this study, we evaluated whether asthma status affects protective vaccine responses with homologous and heterologous protection, using a house dust mite (HDM)-induced chronic asthma mouse model. HDM is an important indoor allergen in humans. The HDM mouse model closely resembles the features of human allergic asthma, such as airway hyper-responsiveness and remodeling, increased HDM-specific serum IgE levels, eosinophilic bronchitis, and increased levels of inflammatory cytokines, including interleukin (IL)-4 and IL-13. It is widely used in asthma research to investigate underlying mechanisms and explore treatment options

[15–17]. Furthermore, we assessed the effects of AddaVax™, which is equivalent to the MF59 adjuvant, on the vaccine efficacy in asthmatic mice. MF59 is a safe and effective squalene oil-in-water vaccine adjuvant used as an influenza vaccine for immunocompromised individuals, such as the elderly, children, and pregnant women [18]. Our study contributes to the understanding of vaccine immunity in asthma, and offers insights into potential developmental strategies.

Method

Induction and confirmation of HDM induced asthma mice model

Six-week-old female BALB/c mice were purchased from Orient Bio and maintained at Jeju National University Animal Facility. The BALB/c mouse model of HDM-induced chronic allergic asthma was used in this study [19]. 25 µg of house dust mite (*Dermatophagoides pteronyssinus*) extract (Stallergenes Greer) were resuspended in 35 µL of PBS and intranasally delivered to mice 5 days per week. Control or naïve groups were intranasally administered 35 µL of PBS without HDM extract. Mice were challenged up to six weeks. Asthma mice were sacrificed at 6 weeks after induction and their asthma features were evaluated. Experiment was done twice with qualitatively similar outcomes. As an indicator of the allergic response, the levels of immunoglobulin E (IgE) in the sera and the population of eosinophils in the lung and bronchoalveolar lavage fluid (BALF) were measured. The population of inflammatory cells in the lungs and BALF, levels of inflammatory cytokines and chemokines, and hematoxylin and eosin (H&E)-stained histological features of lung tissues were analyzed to evaluate lung inflammation. To investigate the properties of T cells in asthmatic mouse, the expression of the T cell exhaustion marker, thymocyte selection-associated HMG BOX (TOX) and programmed cell death receptor-1 (PD-1) were determined using flow cytometry [20, 21]. HDM-specific IFN-γ and IL-4 cytokine-producing T cell percentages were measured after re-stimulation with the HDM extracts.

Split influenza vaccine and viruses

The human influenza virus strain A/Puerto Rico/8/1934 H1N1 (A/PR8) was obtained from ATCC (VR-95™) and amplified in 9-day old embryonated chicken eggs. The virus was harvested from allantoic fluid. To produce the split vaccine, the allantoic fluid was inactivated with 1% neutralized buffered formalin overnight at 4 °C. The virus was purified by ultracentrifugation for 1 h at 30,000 rpm to obtain an inactivated virus. After incubation with 1% Triton X-100 for 2 h at 4 °C to fragment the virus, the

virus was transferred to a dialysis cassette and washed five times with PBS. The split A/PR8 virus vaccine and live A/PR8 virus were maintained at -80°C until use.

Vaccine immunization and virus challenge

Mice were divided into six groups ($n=12/\text{group}$): naïve, naïve A/PR8 vaccine (naïve vac), naïve A/PR8 vaccine AddaVax™ adjuvant (naïve vac AddaVax™), asthma, asthma A/PR8 vaccine (asthma vac), and asthma A/PR8 vaccine AddaVax™ adjuvant (asthma vac AddaVax™). Vaccine groups were intramuscularly vaccinated twice at 4 and 6 weeks after asthma induction at a dose of $1\ \mu\text{g}$ of split A/PR8 vaccine with or without AddaVax™. For immunization and infection, the mice were anesthetized using isoflurane. Sera were collected at 13 days after the prime vaccination and 14 days after the boost vaccination to measure vaccine-specific immunoglobulin levels and hemagglutination inhibitory titers.

Mice were sacrificed at three different time points ($n=4/\text{group}$): (1) 2 weeks after the boost vaccination (2) 5 days after homologous infection (3) 10 days after homologous infection.

At 2 weeks after the boost vaccination, memory antibody production function of plasma cells (bone marrow) and memory B cells (spleen) were measured. At 2 weeks after the boost vaccination, mice were challenged intranasally with live A/PR8 virus (H1N1, at a dose of $2.5\ \text{LD}_{50}$) to determine homo protection. The LD_{50} of the A/PR8 viral stock was determined using preliminary mouse viral challenge experiments. 5 days after viral infection, mice were sacrificed to evaluate the pathogenesis of influenza. Viral titers were determined as the 50% egg infectious dose (EID_{50})/mL. After monitoring the daily body weight change and survival for 10 days after infection, mice were sacrificed and T cell populations in lung and spleen cells were measured. Experiment was done twice with qualitatively similar outcomes. The immunization and infection schedules are shown in Supplementary Fig. 1.

Sample collection and preparation

Sera were harvested via centrifugation of blood collected from the caudal vena cava. BALF samples were collected by delivering 1.2 mL PBS through the trachea using a 25-gauge catheter. Lung tissues were obtained separately for histological and cellular/cytokine analysis. For histological analysis, the lung tissues were immediately fixed with 10% formalin. Lung tissues for cellular/chemical analysis were mechanically mashed and filtered using a 100- μm cell strainer. Following centrifugation, the supernatants were stored at -80°C until cytokine enzyme-linked immunosorbent assay (ELISA). Following red blood cell lysis, the lung cell pellets were resuspended

in 1 mL PBS containing 2% fetal bovine serum (FBS, FACS buffer) for flow cytometry. Lung extracts for virus titration were stored at -80°C until use.

Serum antigen-specific ELISA

To measure A/PR8-specific IgG, IgG1, IgG2a, and HDM-specific IgE levels in the serum, the ELISA plate was coated with inactivated PR8 vaccine or HDM protein (400 ng/well) before adding the serum. Serially diluted sera were added to antigen-coated ELISA plates after blocking. Horseradish peroxidase (HRP)-labeled anti-mouse IgG, IgG1, IgG2a, and IgE secondary antibodies (Southern Biotech) were used to detect antigen-specific immunoglobulins in the serum. Tetramethylbenzidine solution was used as the substrate, and the reaction was stopped using sulfuric acid. Optical density was measured at 450 nm.

Plasma cell, memory B cell antigen-specific immunoglobulin ELISA

The A/PR8 coated plates were blocked with 10% fetal bovine serum containing RPMI 1640 medium for 1 h at room temperature to measure the memory B cell response to the influenza virus. Bone marrow and spleen cells were collected at 7 days post-infection, seeded at a density of 2×10^6 cells/mL onto the plates, and then incubated at 37°C for 1 or 5 days. Anti-mouse IgG, IgG1, and IgG2a antibodies were used to detect influenza-specific antibodies secreted by the antibody-producing B cells.

Hemagglutination inhibitory (HI) assay

Sera samples were incubated overnight at 37°C with RDE II (DENKA SHEIKEN CO. LTD.) at a 1:3 ratio. The samples were inactivated at 56°C for 30 min and stored at 4°C until further use. The samples were initially diluted tenfold, followed by twofold serial dilutions of up to 1280-fold. Serum samples (25 μL) were incubated with 25 μL of 3 hemagglutination units of A/PR8 virus for 30 min at room temperature. Then, 50 μL of 0.5% chicken red blood cells (RBC) was added to each well and incubated for 30 min at room temperature. The endpoint dilution of HI activity in Chicken RBCs was determined.

Cytokine and chemokine ELISA

Cytokines in the BALF and lung extracts were measured using a tumor necrosis factor (TNF)- α , IL-6, IL-12 p40 Mouse Uncoated ELISA Kit (Invitrogen), and interferon (IFN)- γ , IL-4, granzyme B DuoSet ELISA kit (R&D Systems) according to the manufacturer's protocols.

Flow cytometry

For cell phenotype staining, the Fc receptors of the harvested cells were blocked using anti-CD16/32 (clone 2.4G2) antibody after washing with FACS buffer. Each antibody cocktail was then added to the cells and incubated for 30 min at room temperature in the dark. Intracellular cytokine staining for TOX, IL-4, and IFN- γ was performed using a BD Cytofix/Cytoperm kit. To measure IL-4 and IFN- γ cytokine-producing T cells, cells were incubated for 4 h with 5 μ g/mL of antigen (HDM or split A/PR8) after treatment with Golgi-stop.

Table 1 List of antibodies used in flow cytometry analysis

	Antibody for flowcytometry
Inflammatory cell	anti-mouse CD45 (clone 30-F11) CD11b (clone M1/70) CD11c (clone N418) F4/80 (clone BM8) Ly6c (clone AL-21) MHC class II (clone I-A/I-E) CD170 (clone S17007L) Live/dead aqua (L/D)
Memory T cell	anti-mouse CD45 (clone 30-F11) CD3 (clone 17A2) CD4 (clone RM4.5) CD8a (clone 53-6.7) CD44 (clone IM7) CD62L (Clone MEL-14) Live/dead aqua (L/D)
Exhausted T cell	anti-mouse CD45 (clone 30-F11) CD3 (clone 17A2) CD4 (clone RM4.5) CD8a (clone 53-6.7) PD-1 (Clone 29F.1A12) TOX (Clone TXRX10)
Intracellular cytokine	anti-mouse CD45 (clone 30-F11) CD3 (clone 17A2) CD4 (clone RM4.5) CD8a (clone 53-6.7) IL-4 (Clone 11B11) IFN- γ (Clone XMG1.2)

Data were acquired using a BD LSR Fortessa at the Bio-Health Materials Core Facility, Jeju National University, and analyzed using FlowJo software. Table 1 lists the antibodies used in this study and the gating strategy is shown in Supplementary Fig. 2.

Histopathological examination of mice lung

Portions of the left lower lobe lung tissue were fixed in 10% neutralized buffered formalin, processed, and embedded in paraffin. Sections were cut in 4 μ m of thickness and stained with H&E. Lung Sections (15–20 photos per group) were scored from 0–4 blindly by three researchers for bronchial lesions and alveolar lesions using an adapted histological scoring system (Table 2) that was originally described by Dubin et al. [22]. To determine eosinophil infiltration in the lungs, modified Congo Red staining was performed [23].

Lung virus titration

The lung extracts from the influenza-infected mice groups were serially diluted in PBS from 10^{-2} to 10^{-12} , and 300 μ L of each dilution was inoculated into 9-day old embryonated chicken eggs (three eggs per dilution). After incubation for three days, 50 μ L of allantoic fluid was collected and added to a 96 well U-bottom plate. 50 μ L of 0.5% RBC was added to each well and incubated for 30 min at room temperature. The 50% endpoint for hemagglutinin activity in chicken RBC was determined according to the method of Reed and Muench [24].

Statistical analysis

All results are presented as mean \pm standard error of the mean, and statistical significance was analyzed using GraphPad Prism software 10.09 (GraphPad Software Inc.). Significant differences between two groups were

Table 2 Lung inflammation scoring of mice after influenza infection

Score	Bronchiolar Infiltrate		Alveolar involvement
	Intraluminal infiltrate	Peri bronchial Infiltrate	
0	None	None	None
1	\leq 25% of visualized lumens; inflammatory cell exudates and pre-dominate mononuclear	Infiltrate \leq 4 cells thick	Slight increase of cellularity
2	25–50% of visualized lumens; inflammatory cell exudates and mixed mono- and polymorphonuclear	Infiltrate 5–10 cells thick	Moderate increase of cellularity
3	50–75% of visualized lumens; inflammatory cell exudates and predominately polymorphonuclear	25–50% of visualized lumens	Significant increase of cellularity, thickening; obliteration of < 50% of visualized alveolar space
4	Diffuse; inflammatory cell exudates and predominately polymorphonuclear	Diffuse	Obliteration of > 50% of the alveolar space

analyzed using unpaired t-test. One-way ANOVA or two-way ANOVA was used for the comparison of multiple groups. Statistical significance was set at $p < 0.05$.

Result

A 6-week HDM-induced asthma mice model showed typical features of chronic allergic asthma

To establish a HDM mouse model, mice were sensitized and challenged intranasally 5 days per week for up to 6 weeks with 25 μg of HDM extract suspended in 35 μl of PBS. Asthma mice successfully represented the features of allergic asthma. They also showed increased serum levels of HDM-specific IgE, TNF- α , IL-12p40, and IL-4 (Fig. 1A–D) in the lung, as well as representative broncho-pathological characteristics, such as inflammatory cell infiltration around the bronchus and blood vessels, and mucous plugging. They also exhibited structural changes such as airway thickening, smooth muscle thickening, and increased alveolar cellularity in lung histology (Fig. 1E, F). The population of infiltrated inflammatory cells was determined using flow cytometry. A significant increase in the number of eosinophils, monocytes, neutrophils, and dendritic cells (DC) was observed in the lungs and BALF of asthma mice. The number of eosinophils, monocytes, neutrophils, and DC in the lungs and BALF increased in asthmatic mice (Fig. 1G, H). Among the inflammatory cells, the population of eosinophils showed the largest increase in the lungs (Fig. 1I). In addition, we analyzed the population of T cell subsets in asthma mice. They showed an increase in the population of effector memory CD4⁺ T cells (Fig. 2A, B, C) in the lungs. However, the percentages of IFN- γ or IL-4 cytokine-producing CD4⁺ T cells in the lungs after HDM restimulation were lower than those in the control (Fig. 2A, D, E). Instead, the percentages of exhausted CD4⁺ and CD8⁺ T cells in the lungs were significantly increased in asthma mice (Fig. 2A, F, G).

Asthma mice exhibited lower serum HI titer compared to naïve mice after split A/PR8 vaccination, and AddaVaxTM adjuvant enhanced antibody response and HI titer against A/PR8 in both naïve and asthma mice

To investigate vaccine efficacy in asthma, mice were immunized twice with a split A/PR8 vaccine, with or without AddaVaxTM supplementation. The level of sera IgG, and IgG1 were increased after prime and boost vaccination in both naïve and asthma mice. There was no significant difference in the antibody levels between the naïve and asthma vac groups (Fig. 3A–F). AddaVaxTM adjuvant effectively enhanced the levels of IgG and IgG1, but not IgG2a (Fig. 3A–F). The level of IgG1 was slightly lower in the asthma vac AddaVaxTM group than in the naïve vac AddaVaxTM group after boost vaccination (Fig. 3A, B).

We also assessed the antibody-producing capacity of the plasma cells in the bone marrow and memory B cells in the spleen. Split A/PR8 vaccine alone did not significantly enhance antibody-producing cell responses after vaccination. AddaVaxTM supplementation significantly increased IgG production in the bone marrow (Fig. 3G), and spleen cells (Fig. 3H). There was no difference in the levels between naïve and asthma mice.

Although the naïve and asthma vac groups exhibited similar levels of A/PR8-specific serum IgG and IgG1, they showed large differences in the serum HI titer. The naïve and asthma vac AddaVaxTM groups showed the highest dilution titer, followed by the naïve vac group, whereas the asthma vac group remained undetectable (Fig. 3I).

Asthma mice showed reduced vaccine protection against homologous A/PR8 virus challenge, which was effectively compensated for using the AddaVaxTM adjuvant

To evaluate the efficacy of the split A/PR8 vaccine and AddaVaxTM adjuvanted vaccine in asthma mice, mice were challenged with 2.5 LD₅₀ of A/PR8 H1N1 at 2 weeks after boost vaccination. Naïve mice showed good protection after vaccination with or without AddaVaxTM, with no weight loss (Fig. 4A), 100% survival (Fig. 4B), and significantly reduced the viral titer in the lungs at 5 days

(See figure on next page.)

Fig. 1 Evaluation of asthma features of HDM-induced asthma mouse model. Sera and lung samples were collected at 6 weeks post HDM sensitization. **A** HDM-specific IgE levels in the sera were measured using ELISA. **B–D** Inflammatory cytokine levels in the lungs were measured by ELISA. **E, F** Lung tissues were stained with H&E, and representative histological analyses of each group at magnification $\times 200$ and $\times 400$ are shown. **G, H** Frequencies of inflammatory cells in lungs and BALF were measured using flowcytometry. **I** Percentages of inflammatory cells in lungs were shown as parts to whole. Data were shown in mean \pm SEM. For statistical analysis, two-way ANOVA and unpaired t test was performed.

* $p < 0.05$; ** $p < 0.01$; *** $p < 0.001$ **** $p < 0.0001$ between the indicated groups ($n = 4/\text{group}$)

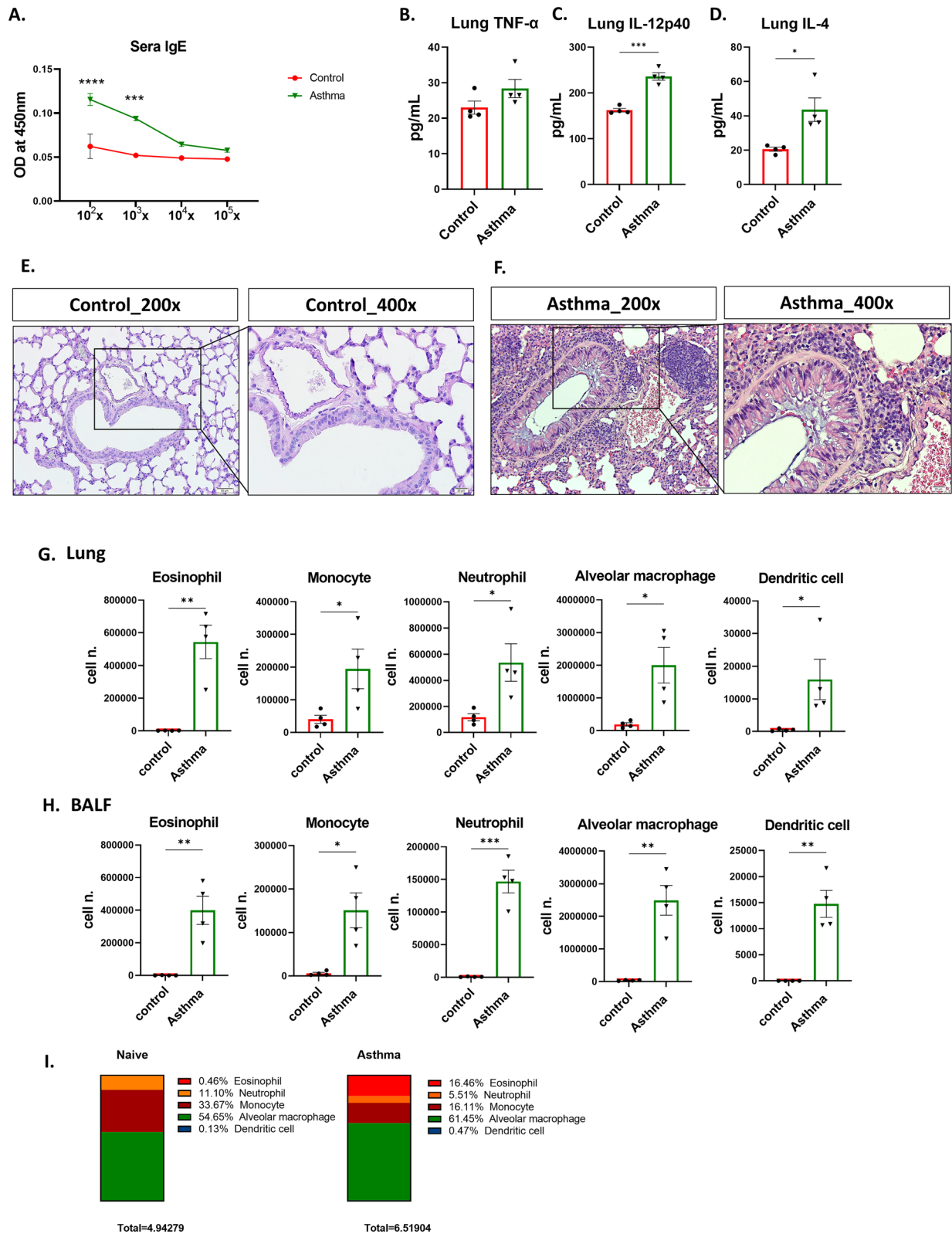


Fig. 1 (See legend on previous page.)

A. Population of T cell subsets in lung after HDM - stimulation

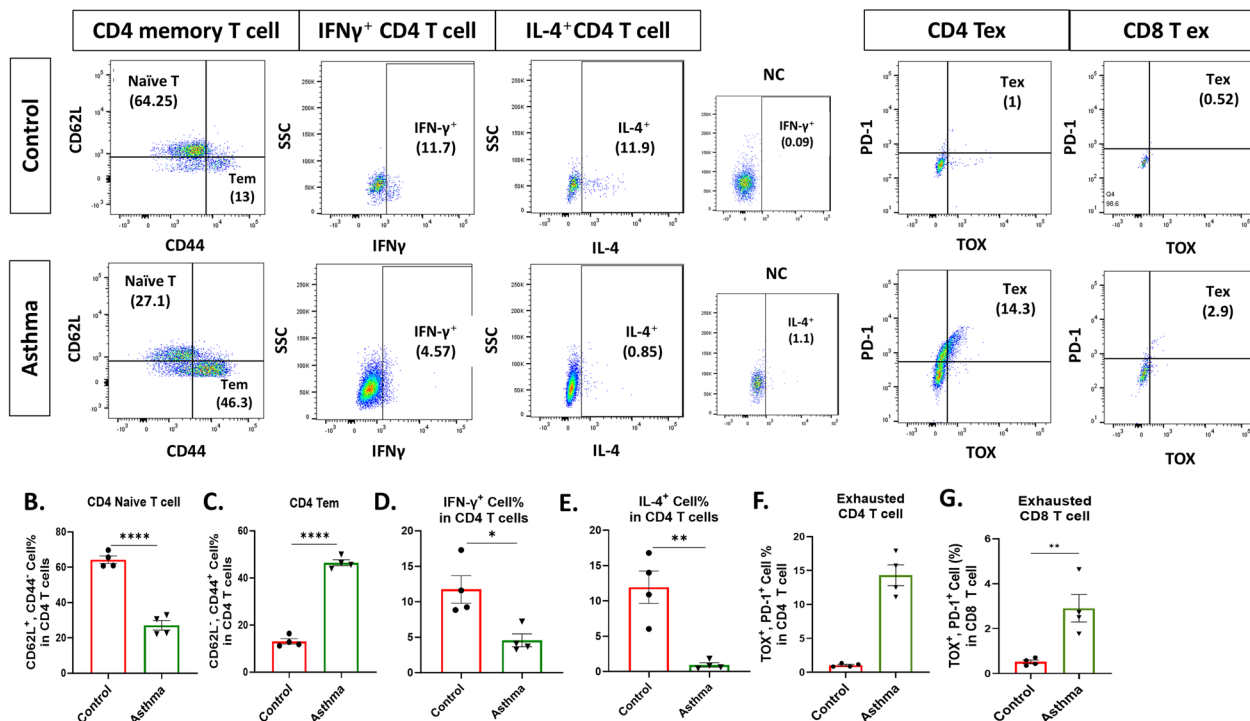


Fig. 2 Evaluation of HDM-specific T cells and exhausted T cell populations in asthmatic mouse lungs. Lung samples were collected at 6 weeks post HDM sensitization. Golgi-stop was treated to cells and cells were re-stimulated for 4 h at 37 °C with HDM extract (5 μ g/mL). T cell populations in the lungs were measured using flow cytometry. **A** Gating strategy and representative data were shown. **B–G** Frequencies of each T cell population were shown. Data were shown in mean \pm SEM. For statistical analysis, unpaired t test was performed. * $p < 0.05$; ** $p < 0.01$; *** $p < 0.001$ **** $p < 0.0001$ between the indicated groups (n = 4/group)

post-infection compared to that in the naïve infection (inf.) group (Fig. 4C). The asthma mice also showed better protection after A/PR8 split vaccination with 100% survival (Fig. 4B) and reduced viral titer (Fig. 4C) in the lungs than the asthma infected mice. However, the asthma vac inf. group showed significant weight loss (Fig. 4A) and higher virus titer (Fig. 4C) compared with the naïve vac inf. groups, whereas the asthma vac AddaVaxTM inf. group was fully protected, with no weight loss (Fig. 4A), and a low viral titer, which was even lower than that of the naïve vac AddaVaxTM inf. group (Fig. 4C).

AddaVaxTM augmented eosinophil infiltration after homologous virus challenge at the site of infection and increased A/PR8 specific IgE level in lung of asthma mice

To further determine the protective effect of the vaccine against A/PR8 virus challenge in asthma mice, inflammatory cytokine levels, inflammatory cell populations in the airway, and histopathology of the lung tissues were determined at 5 days post-infection. In lung, naïve vac inf. and vac AddaVaxTM inf. groups showed decreased levels of IL-6 and granzyme B compared to

those in the naïve inf group. Asthma inf. group showed higher level of TNF- α , IL-6, and IFN- γ than in the naïve inf. group. Asthma vac AddaVaxTM inf. group showed decreased levels of TNF- α , IL-6, IFN- γ , and granzyme B compared with the in those asthma group. Asthma vac inf. group showed decreased level of TNF- α , and IL-6. IL-4 level was higher in the asthma group than in the control group. In addition, it showed higher levels of IL-6, IFN- γ , IL-4, and granzyme B than asthma vac AddaVaxTM inf. group (Fig. 5A). In BALF, the levels of TNF- α , IL-6, and IFN- γ among the groups exhibited a pattern consistent with that observed in the lungs. The level of IL-4 increased in naïve vac AddaVaxTM inf. group compared to the naïve inf. and asthma vac AddaVaxTM inf. group. Asthma vac inf. group showed the highest levels of granzyme B among the groups (Fig. 5B).

The percentage of eosinophils, neutrophils, monocytes, alveolar macrophages, and dendritic cells in the lungs (Fig. 5C), and BALF (Fig. 5D) was measured using flow cytometry. Both the naïve vac inf. and the naïve vac AddaVaxTM inf. groups exhibited significantly decreased percentages of monocytes and neutrophils in the lungs compared to those in the naïve infection group (Fig. 5C).

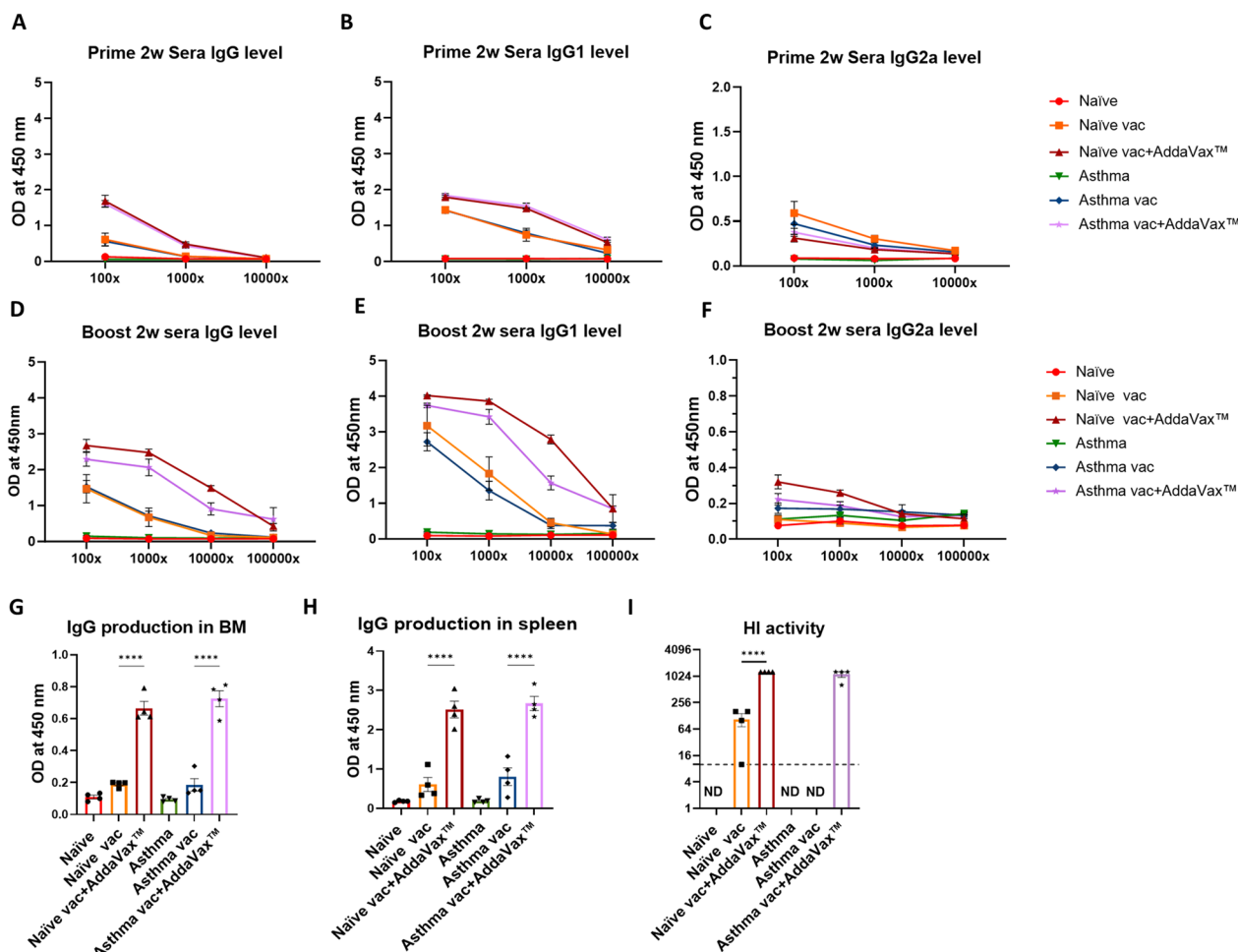


Fig. 3 A/PR8-specific antibody production after prime and boost vaccination. Serum samples were collected at 2 weeks after prime and boost vaccination. Sera Ig G, G1, G2a levels were measured using ELISA (A–F). Bone marrow (BM) cells and spleen cells were collected at 2 weeks after boost vaccination and cultured in A/PR8 pre-coated 96 well cell-culture plate for 1 day (BM) and 7 days (spleen). Memory Ig G response in the (G) bone marrow and (H) spleen were measured using ELISA. 2 weeks post boost vaccination serum samples were initially diluted tenfold, followed by twofold serial dilutions of up to 1280-fold and incubated with 3 HA unit of A/PR8 virus. I The endpoint dilution of HI activity in Chicken RBCs was determined. Data were shown in mean ± SEM. For statistical analysis, two-way ANOVA (A–F) and one-way ANOVA (G–I) were performed. ****p < 0.0001 between the indicated groups (n = 4/group)

In BALF, naïve vac inf. group exhibited high levels of monocytes and neutrophils, whereas the naïve vac AddaVax™ inf. group exhibited a significant decrease in these cell populations (Fig. 5D). In asthma mice, however, the vac inf. group did not show a significant decrease in the populations of monocytes and neutrophils in the lung and BALF, whereas the vac AddaVax™ inf. group showed a substantial decrease in monocyte populations (Fig. 5C, D). The tendency of inflammatory cell populations was similar in the cell number graphs (Sup. 3).

We also evaluated the histopathology of lung tissues using H&E staining. Representative photos were selected based on the mean inflammation score (Fig. 6A, B). The lungs of the naïve inf. group showed moderate

infiltration of inflammatory cells around the bronchioles and blood vessels, with some debris of cells inside the lumen (bronchiole score, 1.8). Cellularity in the alveolar space moderately increased (alveolar score, 2.1). The severity of inflammation in naïve vac inf. group was considerably lower than that of the naïve inf. group (bronchiole score 0.5, alveolar score 0.9). The severity of inflammation in naïve vac AddaVax™ inf. group was increased in both bronchiole and alveolar, showing similar score (bronchiole score 1.8, alveolar score 2.7) to naïve inf. group. The asthma inf. group showed severe inflammatory cell infiltration in the bronchiole region and narrowing of the lumen by mucus and cell debris (bronchiole score, 2.6). They also had significantly

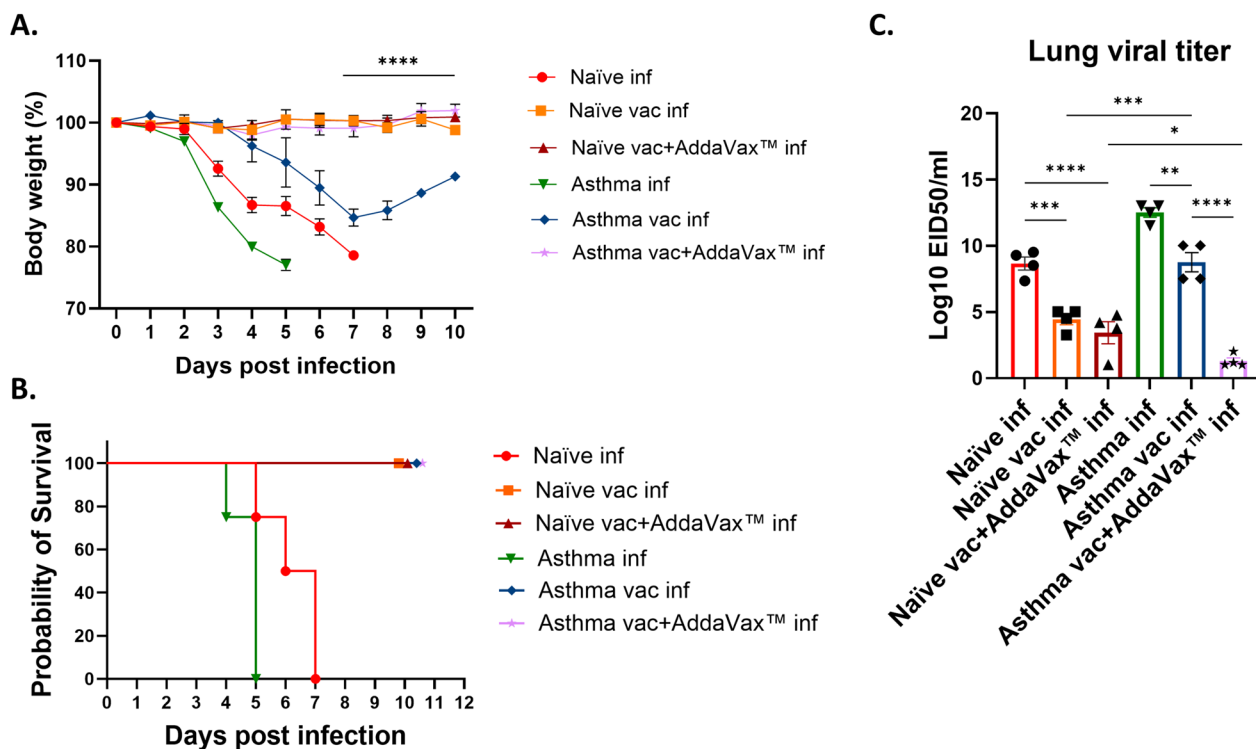


Fig. 4 Determination of homologous protective efficacy of the A/PR8 split vaccine with or without AddaVax™ in naïve and asthma mice. **A** Body weight changes were monitored for 10 days after infection with A/PR8 influenza virus (2.5 LD₅₀). **B** Survival rate of the asthma mice after infection with A/PR8 virus. **C** Lungs were collected at day 5 post infection and viral titers were determined in EID₅₀/mL. All data were shown in mean ± SEM. For statistical analysis, two-way ANOVA was performed for body weight change. ****p < 0.0001 between asthma vaccine group and naïve group. One-way ANOVA was performed for virus titer. *p < 0.05; **p < 0.01; ***p < 0.001; ****p < 0.0001 between the indicated groups (n = 4/group)

increased alveolar cellularity and obliteration of the alveolar space (alveolar score 3.2). Inflammation scores of the asthma vac inf. group (bronchiole score 2.4, alveolar score 2.7) were less severe than those of the asthma infection group, but showed higher bronchiole score than asthma group. Asthma vac AddaVax™ inf. group showed lower inflammation scores (bronchiole score 2, alveolar score 2.2) than asthma inf. group, similar score to asthma group.

Increased eosinophil infiltration was confirmed by lung histology staining using modified Congo Red staining. An elevated number of eosinophils (red arrowhead) was detected in the peri-bronchiole/peri-vascular region of the lungs in the naïve and asthma vac AddaVax™ inf. groups compared to the other groups (Fig. 6C). Notably the histopathological features of naïve vac AddaVax™ inf. group were similar to allergic inflammation in lung, showing eosinophil infiltration and airway thickening.

We examined A/PR8-specific IgE levels in BALF and lung to determine if the increased eosinophil level is related with allergic response against A/PR8 virus. A/PR8-specific IgE level in BALF were elevated in asthma groups but were only statistically significant in the

asthma inf. group. A/PR8-specific IgE level in lung were significantly increased in asthma vac AddaVax™ inf. group (Fig. 6D).

Asthma groups exhibited higher percentage of DN cell populations compare to same treated condition naïve groups after infection

We assessed T cell populations in the lung and spleen at 10 days post infection. Following vaccination, we noted an increase in the percentage of CD4⁺ T cell populations in CD3⁺ cell population, whereas the percentage of CD4, CD8 double negative (DN) cell populations decreased in the lung and spleen of naïve and asthma mice (Fig. 7A, B). Also, the percentage of CD4⁺ T cell population was higher in naïve inf. group compare to the asthma inf. group. In lung, the percentage of CD8⁺ T cell populations was higher in naïve vac inf. group compare to asthma inf. group. The percentage of DN cell populations was higher in asthma groups compare to same treated condition naïve groups (Fig. 7A). In spleen, the percentage of CD4⁺ T cell population was lower and the percentage of DN cell populations was higher in asthma groups compare to same treated condition naïve groups. The percentage of

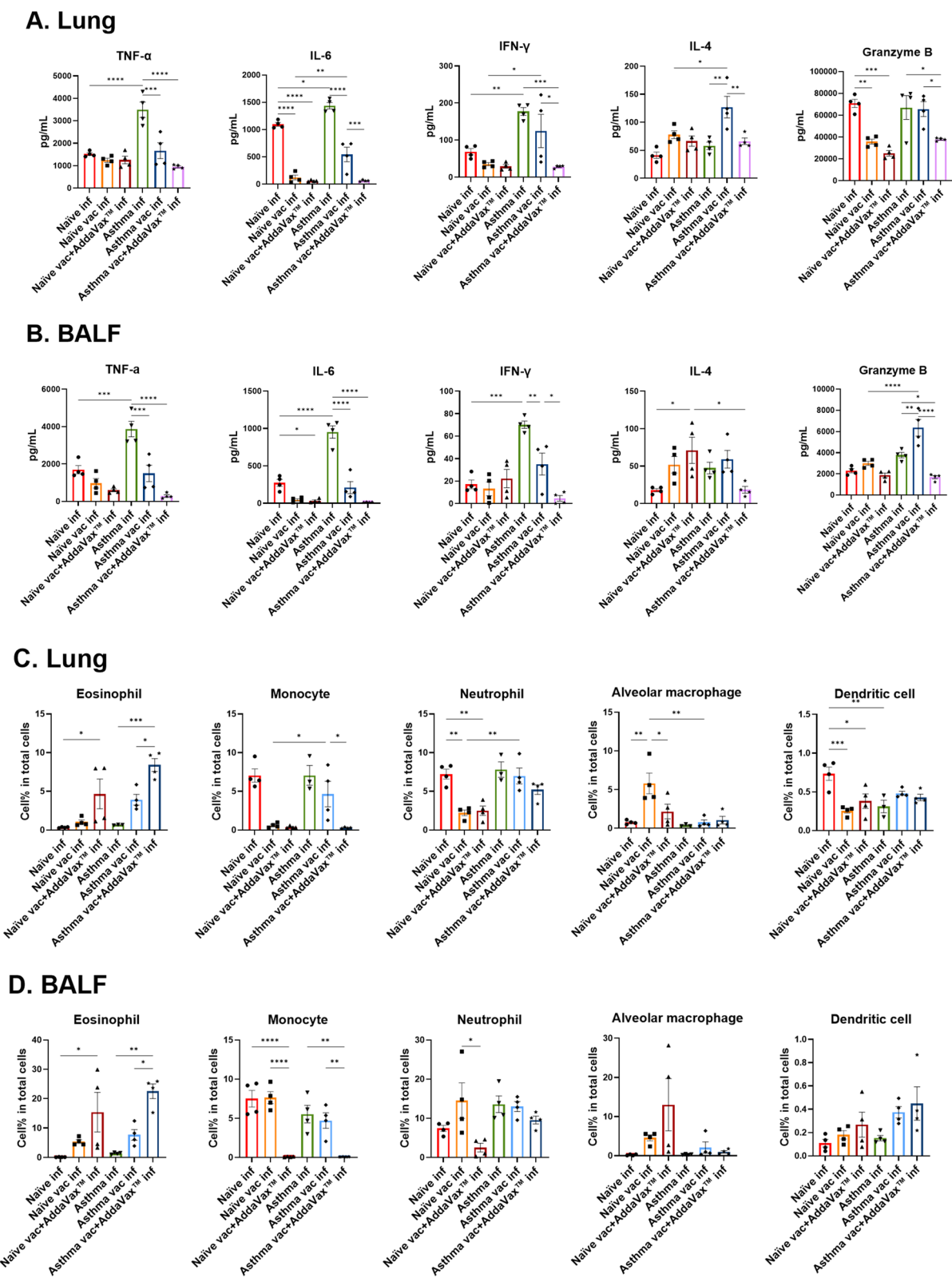


Fig. 5 Inflammatory cytokine levels and cell infiltration in the lungs and BALF after A/PR8 challenge. Lung samples were collected at 5 days post infection. Inflammatory cytokine levels in the lung (A) and BALF (B) were measured by ELISA. Inflammatory cell populations in the lung (C) and BALF (D) were measured by Flow cytometry. All data were shown in mean ± SEM. For statistical analysis, one-way ANOVA was performed. *p < 0.05; **p < 0.01; ***p < 0.001; ****p < 0.0001 between the indicated groups (n = 4/group)

CD8⁺ T cell populations was higher in asthma inf. group than naïve inf. group and asthma vac inf. group compared to the naïve vac inf. group (Fig. 7B).

Discussion

Asthma is a significant disease affecting 300 million people worldwide and increases the risk of hospitalization for the influenza virus [25]. The danger stems not only from lung malfunction and asthma exacerbation [26, 27] but also from the potential alteration in immunity due to chronic inflammation [28]. Our previous study demonstrated T cell exhaustion in asthma condition [11], and Huilei Zhang et al. found effector memory CD8 T cell dysfunction in asthma conditions [29], raising concerns about the efficacy of influenza vaccines.

Previous studies have investigated the impact of asthma on vaccine efficacy using a mouse model; however, this has been controversial [30–32]. Here, we demonstrated a clear reduction in the protective efficacy of split A/PR8 vaccination against homologous influenza infections in the asthma condition, whereas the vaccination provided complete protection in normal mice at the same dosage. 6-week HDM exposure increased the Th 2 response and T cell exhaustion.

The viral challenge dose of 2.5 LD₅₀ in this study was effectively mitigated by high antibody levels and HI activity in the naïve vac AddaVax™ group, as evidenced by reduced recruitment of monocytes and neutrophils and low levels of IFN-γ and granzyme B. The naïve vac group exhibited lower antibody levels and HI activity compared to the naïve vac AddaVax™ group. Consequently, activation of cellular immunity appeared necessary for viral clearance, as indicated by the recruitment of monocytes and neutrophils in BALF. The naïve group was unable to withstand the 2.5 LD₅₀ viral challenge.

The efficacy of vaccine in asthma mice were similar to that in naïve mice when considering survival rates. However, we could find differences in some details between asthma and naïve mice after vaccination. First, serum HI assay showed that HI activity of asthma vac group was substantially lower than naïve vac group, although total serum IgG and IgG1 level was not differ between groups. This is an important finding which

might contribute to increased body weight loss and viral titer after challenge in asthma vac inf. group. One possibility is a reduction in antibody affinity, which still bind to influenza antigens but have weaker neutralizing activity. If the chronic HDM antigen exposure depleted the naïve B cell pool in secondary lymphoid organs in asthma mouse, it may lead to the reduction of competition among B cells. This diminished competition can impair the selection of high-affinity memory B cells and plasma cells, ultimately lowering the average antibody affinity. Another possible explanation is a shift in the antibody response away from HA toward internal viral proteins such as nucleoprotein (NP) or matrix protein 1 (M1) by asthma induced inflammation. However, since split-virus vaccines primarily contain HA and NA, with only minimal amounts of NP and M1 (as most internal components and egg proteins are removed during the chemical processing) [33], it is unlikely that asthma-induced inflammation would significantly redirect the antibody response toward these internal proteins, although it remains a possibility worth considering. Lastly, it's another low possible explanation, that the presence of an expanded population of HDM-induced memory B cells in asthma mice may contribute to the production of antibodies targeting non-neutralizing regions of HA or NA, such as glycan structures rather than receptor-binding sites, which shares a common structure with HDM antigens. This could reduce the proportion of antibodies capable of effectively blocking viral entry, thereby lowering HI titers.. Second, in both lung and spleen, the percentages of DN cell populations were higher in asthma groups compare to same treated condition naïve groups. Possible cell types in this population are double-negative NKT cells and double-negative T cells (DNT) [34, 35]. DNT cells can have memory functions and can expand and activate against pathogens. It is a minor subset of T cells but is associated with multiple disease conditions [36–40]. This study had limitations in distinguishing these cell types. Nevertheless, this result suggests that asthma mice have alternative immune cell populations when responding to viral challenges. Further research investigating the actions of underrepresented immune cell subsets in asthma mice model, including mast cells,

(See figure on next page.)

Fig. 6 Lung histopathological analysis and A/PR8-specific Ig E level in BALF and lung after A/PR8 challenge. The representative histology pictures of lung tissues at magnification ×200 (A) and the inflammation score in lung (B) after A/PR8 influenza virus infection. Lung tissues were collected at 5 days post infection and stained with H&E. The lung inflammation score was blindly quantified (15–20 pictures/group) between 0–4. C Representative histological photos of lung tissues at magnification of ×400 and ×1000, stained with Congo red. D A/PR8-specific IgE levels in BALF and lungs were measured by ELISA. The lung inflammation score graph and IgE level data were shown in the mean ± SEM. For statistical analysis, one-way ANOVA was performed. *p < 0.05; **p < 0.01; ***p < 0.001; ****p < 0.0001 between the indicated groups

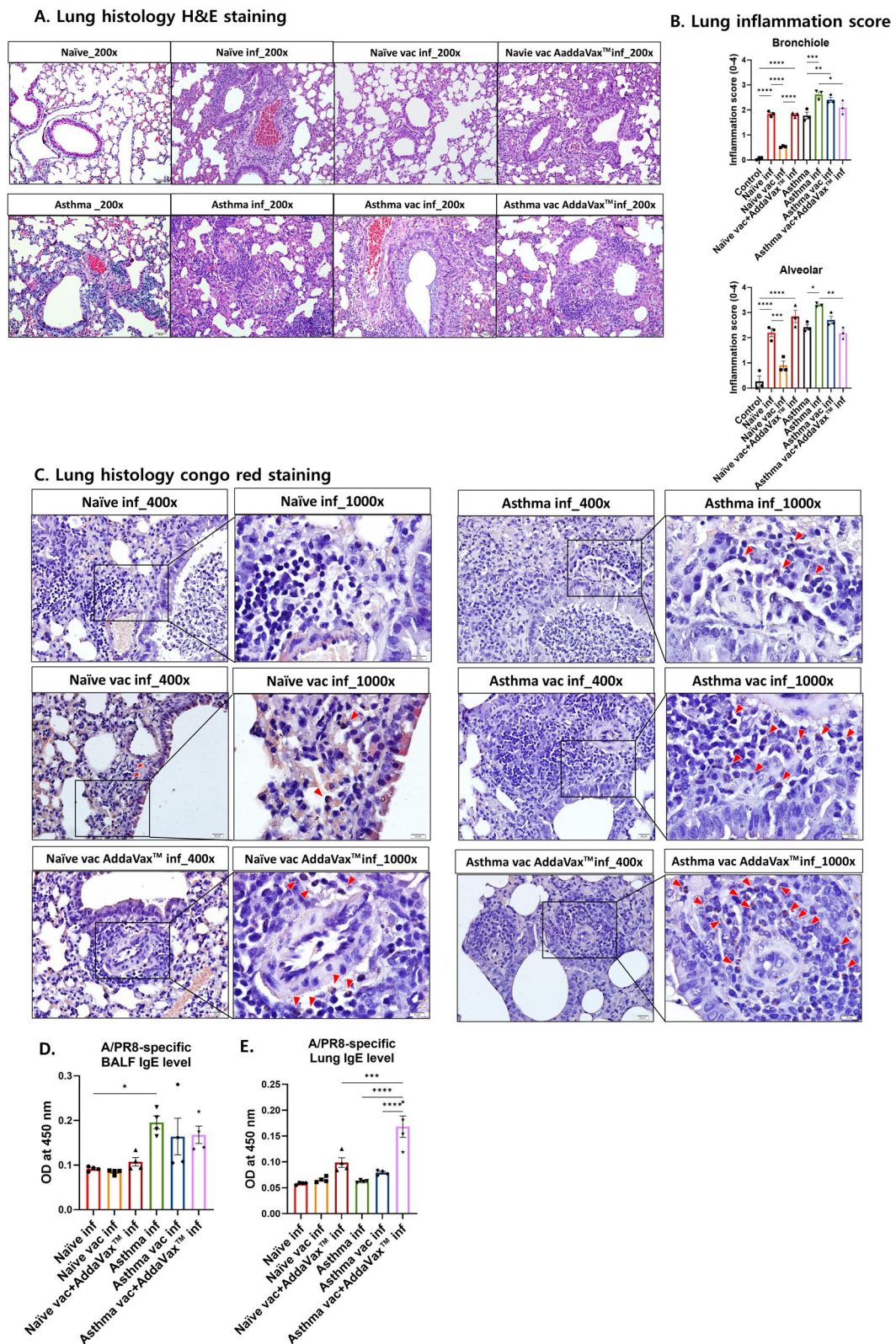


Fig. 6 (See legend on previous page.)

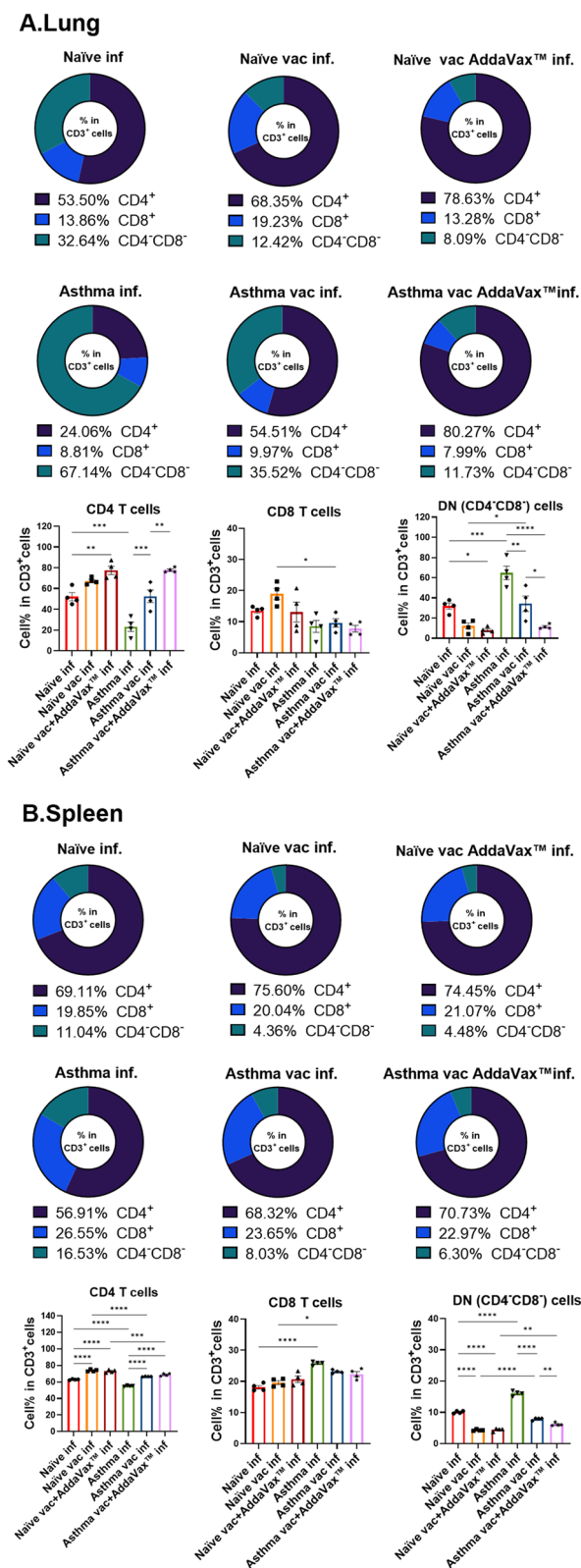


Fig. 7 T cell populations in the lung and spleen at 10 days after infection after A/PR8 re-stimulation. Lung and spleen cells were collected at 10 days after infection. Cells were incubated for 4 h at 37 °C with A/PR8 peptide (5 µg/mL). T cell populations in the lung (A-D) and spleen (E-H) were measured by flow cytometry. All data were shown in mean ± SEM. For statistical analysis, one-way ANOVA was performed. *p < 0.05; **p < 0.01; ***p < 0.001; ****p < 0.0001 between the indicated groups (n = 4/group)

NK cells, NK T cells, and basophils, may enhance the understanding the action of asthma immunity against virus and reproducibility of the model.

Despite asthma’s pathological feature of a Th 2 skewed immune response, upon exposure to a lethal dose of influenza virus infection, subjects typically elicit an anti-viral response characterized by elevated levels of IFN-γ and granzyme B. IFN-γ is primarily secreted by Th-1 CD4⁺ T cells [41, 42], cytotoxic CD8⁺ T cell [43], NK cell [44], and NKT cell [45, 46]. Granzyme B is mainly secreted by NK cell [47, 48], NKT cell [49], cytotoxic CD8 T cell [50, 51] and also mast cell [52]. Furthermore, inflammation was associated with the activation of monocytes and neutrophils rather than eosinophils. Study of Sujin An et al. showed that at the initial stage of infection asthma mice can control viral replication via rapid induction of type III IFN. However, asthma mice become vulnerable to infection after 7 days and intranasal administration of type III IFNs increased the protection [53]. This suggests that asthma mice can also respond normally to the virus, but there are limitations in their immune ability to maintain IFN-mediated immune activation for antiviral responses and consequently exhibit increased susceptibility.

Therefore, the elevated eosinophil levels observed in the vac AddaVax™ groups can be attributed solely to the vaccine’s effects. In both naive and asthma mice, AddaVax™ adjuvanted vaccination enhanced serum A/PR8-specific antibody level and HI activity and significantly reduce lung viral titer. However, both of groups exhibited significant eosinophil recruitment in the lung and BALF after infection. It has been reported that split inactivated influenza vaccines can increase eosinophil levels in lung in mice following viral challenge [54]. Furthermore, the addition of AddaVax™ has been observed to enhance this effect [55].

In this study, naïve vac AddaVax™ inf. group showed acute eosinophilic pneumonia and increased IL-4 level in BALF. It did not show the increase in the level of A/PR8-specific IgE in the lung or BALF. Asthma vac AddaVax™ group displayed an elevation in eosinophil levels but not

in cytokine levels or observable asthma exacerbation in lung. Allergen sensitivity may be diminished in the chronic asthma stage compared to the acute stage [56, 57]. Elevated A/PR8-specific IgE levels in the lung suggest the development of an allergic response to the A/PR8 virus.

An allergic response to viruses is undesirable and has the potential to develop into a serious disease with repeated influenza vaccination or virus infection. Although there are studies about the anti-bacterial and anti-viral actions of eosinophil [58–60], still it is strongly associated with the exacerbation of allergic inflammation [61], and recent reports have highlighted an increase in cases of eosinophilia following COVID-19 vaccination [62–64]. Asthma mice also present an unknown risk, as elevated eosinophil levels did not exacerbate lung inflammation but may systemically affect inflammation in other organs. Therefore, more active vaccine research and development is necessary, considering not only antibody levels and protection outcomes but also unidentified risk factors and long-term effects. Furthermore, existing guidelines for influenza vaccination do not recommend the use of live attenuated vaccines or nasal spray formulations for individuals with asthma, due to the potential risk of triggering an asthma attack. Developing a vaccine for asthma patients that enhances cellular response without exacerbating underlying disease poses a novel challenge, particularly in light of the potential for severe seasonal and pandemic respiratory viruses to emerge.

This study's results are limited to a particular mouse model, with the evaluation focusing on selected cell types only. Also, it has a limitation in fully elucidating the underlying mechanism of vaccine efficacy in asthma condition and identifying the contribution of each factor. To elucidate the mechanisms of asthma immunity against influenza vaccine and virus, further testing, such as antibody affinity assays and monoclonal antibody measurements, would be needed to confirm the mechanism of reduced neutralizing antibody production in split vaccinated asthma mouse. Comprehensive research is required regarding the function of other immune cells under diverse conditions with longitudinal monitoring. Moreover, evaluating various other vaccine formulations will be crucial for advancing vaccine development tailored to asthma patients. Further studies in human subjects are also necessary.

Abbreviations

Th-1	T helper type 1
Th-2	T helper type 2

IL	Interleukin
IgE	Immunoglobulin E
BALF	Bronchoalveolar lavage fluid
H&E	Hematoxylin and eosin
TOX	Thymocyte selection-associated HMG BOX
PD-1	Programmed cell death receptor-1
naïve vac	Naïve A/PR8 vaccine
naïve vac AddaVax™	Naïve A/PR8 vaccine AddaVax™ adjuvant
asthma vac	Asthma A/PR8 vaccine
asthma vac AddaVax™	Asthma A/PR8 vaccine AddaVax™ adjuvant
LD ₅₀	50% Lethal dose
A/PR8	Human influenza virus strain A/Puerto Rico/8/1934 H1N1
EID ₅₀	50% Egg infectious dose
ELISA	Enzyme-linked immunosorbent assay
PBS	Phosphate-buffered saline
FBS	Fetal bovine serum
HRP	Horse radish peroxidase
TNF	Tumor necrosis factor
inf.	Infection
IFN	Interferon
DC	Dendritic cell
DN	Double-negative
DNT	Double-negative T cells

Supplementary Information

The online version contains supplementary material available at <https://doi.org/10.1186/s12931-025-03209-6>.

Additional file 1;Sup.1 Experimental schedule of immunizations and infection

Additional file 2;Sup.2 Gating strategy of immune cell populations with flow cytometry

Additional file 3;Sup. 3 Inflammatory cell infiltration in the lungs and BALF after A/PR8 challenge. The number of inflammatory cells in the lung (A) and BALF (B) at 5 days post infection was measured by Flow cytometry. All data were shown in mean ± SEM. For statistical analysis, one-way ANOVA was performed. *p < 0.05; **p < 0.01; ***p < 0.001 between the indicated groups (n = 4/group)

Author contributions

Conceptualization: S.Y.Ahn, E.J.Ko, Methodology: S.Y.Ahn, E.J.Ko, Validation: S.Y.Ahn, E.J.Ko, Formal analysis: S.Y.Ahn, Investigation: S.Y.Ahn, T.L.Ho, E.J.Ko, Data Curation: S.Y.Ahn, Writing—Original Draft: S.Y.Ahn, E.J.Ko, Writing—Review & Editing: S.Y.Ahn, T.L.Ho, E.J.Ko, Visualization: S.Y.Ahn, E.J.Ko, Supervision: E.J.Ko, Funding acquisition: E.J.Ko.

Funding

This work was supported by a National Research Foundation of Korea (NRF) grant funded by the Korean government (MSIT) (RS-2023-00211504), the Korea Basic Science Institute (National Research Facilities and Equipment Center) grant funded by the Ministry of Education (2020R1A6C101A188) and the Basic Science Research Program to the Research Institute for Basic Sciences (RIBS) of Jeju National University through the NRF, funded by the Ministry of Education (RS-2019-NR040080).

Data availability

All data in the manuscript is available through the responsible corresponding author.

Declarations

Ethical approval

All mouse experiments were performed in accordance with the guidelines of Jeju National University approved by the Institutional Animal Care and Use Committee (protocol number 2021-0051).

Consent to Participate

Not applicable.

Consent for publication

Not applicable.

Competing interests

The authors declare no competing interests.

Author details

¹Department of Veterinary Medicine and Veterinary Medical Research Institute, College of Veterinary Medicine, Jeju National University, Jeju 63243, Republic of Korea. ²Interdisciplinary Graduate Program in Advanced Convergence Technology & Science, Jeju National University, Jeju 63243, Republic of Korea. ³Bio-Health Materials Core-Facility Center, Jeju National University, Jeju 63243, Republic of Korea.

Received: 4 October 2024 Accepted: 28 March 2025

Published online: 10 April 2025

References

- Akinbami LJ, Moorman JE, Liu X. Asthma prevalence, health care use, and mortality: United States, 2005–2009. *Natl Health Stat Report*. 2011;32:1–14.
- Kim HY, DeKruyff RH, Umetsu DT. The many paths to asthma: phenotype shaped by innate and adaptive immunity. *Nat Immunol*. 2010;11(7):577–84.
- Hsieh YA, Hsiao YH, Ko HK, Shen YL, Huang CW, Perng DW, Su KC. House dust mites stimulate thymic stromal lymphopoietin production in human bronchial epithelial cells and promote airway remodeling through activation of PAR2 and ERK signaling pathway. *Sci Rep*. 2024;14(1):28649.
- McKenna JJ, Bramley AM, Skarbinski J, Fry AM, Finelli L, Jain S, Pandemic Influenza AVHIT. Asthma in patients hospitalized with pandemic influenza A(H1N1)pdm09 virus infection—United States, 2009. *BMC Infect Dis*. 2013;13:57.
- Global strategy for asthma management and prevention. Fontana, WI: Global Initiative for Asthma; 2022. Global Initiative for Asthma.
- Patyk M, Obojski A, Sokolowska-Dabek D, Parkitna-Patyk M, Zaleska-Dorobisz U. Airway wall thickness and airflow limitations in asthma assessed in quantitative computed tomography. *Ther Adv Respir Dis*. 2020;14:1753466619898598.
- Eddy RL, Svenningsen S, Kirby M, Knipping D, McCormack DG, Liciskai C, et al. Is computed tomography airway count related to asthma severity and airway structure and function? *Am J Respir Crit Care Med*. 2020;201(8):923–33.
- Chen M, Shepard K 2nd, Yang M, Raut P, Pazwash H, Holweg CTJ, Choo E. Overlap of allergic, eosinophilic and type 2 inflammatory subtypes in moderate-to-severe asthma. *Clin Exp Allergy*. 2021;51(4):546–55.
- Harker JA, Lloyd CM. T helper 2 cells in asthma. *J Exp Med*. 2023;220(6).
- Huang Y, Qiu C. Research advances in airway remodeling in asthma: a narrative review. *Ann Transl Med*. 2022;10(18):1023.
- Ahn SY, Lee J, Lee DH, Ho TL, Le CTT, Ko EJ. Chronic allergic asthma induces T-cell exhaustion and impairs virus clearance in mice. *Respir Res*. 2023;24(1):160.
- Goronzy JJ, Weyand CM. Understanding immunosenescence to improve responses to vaccines. *Nat Immunol*. 2013;14(5):428–36.
- Gao Z, Feng Y, Xu J, Liang J. T-cell exhaustion in immune-mediated inflammatory diseases: new implications for immunotherapy. *Front Immunol*. 2022;13:977394.
- Trombetta CM, Kistner O, Montomoli E, Viviani S, Marchi S. Influenza viruses and vaccines: the role of vaccine effectiveness studies for evaluation of the benefits of influenza vaccines. *Vaccines (Basel)*. 2022;10(5).
- Woo LN, Guo WY, Wang X, Young A, Salehi S, Hin A, et al. A 4-week model of house dust mite (HDM) induced allergic airways inflammation with airway remodeling. *Sci Rep*. 2018;8(1):6925.
- Chen J, Zhou H, Wang J, Zhang B, Liu F, Huang J, et al. Therapeutic effects of resveratrol in a mouse model of HDM-induced allergic asthma. *Int Immunopharmacol*. 2015;25(1):43–8.
- Allgire E, Ahlbrand RA, Nawreen N, Ajmani A, Hoover C, McAlees JW, et al. Altered fear behavior in aeroallergen house dust mite exposed C57Bl/6 mice: a model of Th2-skewed airway inflammation. *Neuroscience*. 2023;528:75–88.
- Ko EJ, Kang SM. Immunology and efficacy of MF59-adjuvanted vaccines. *Hum Vaccin Immunother*. 2018;14(12):3041–5.
- Cassado Ados A, D'Imperio Lima MR, Bortoluci KR. Revisiting mouse peritoneal macrophages: heterogeneity, development, and function. *Front Immunol*. 2015;6:225.
- Khan O, Giles JR, McDonald S, Manne S, Ngwi SF, Patel KP, et al. TOX transcriptionally and epigenetically programs CD8(+) T cell exhaustion. *Nature*. 2019;571(7764):211–8.
- Barber DL, Wherry EJ, Masopust D, Zhu B, Allison JP, Sharpe AH, et al. Restoring function in exhausted CD8 T cells during chronic viral infection. *Nature*. 2006;439(7077):682–7.
- Dubin PJ, Kolls JK. IL-23 mediates inflammatory responses to mucoid *Pseudomonas aeruginosa* lung infection in mice. *Am J Physiol Lung Cell Mol Physiol*. 2007;292(2):L519–28.
- Grouls V, Helpap B. Selective staining of eosinophils and their immature precursors in tissue sections and autoradiographs with Congo red. *Stain Technol*. 1981;56(5):323–5.
- Reed LJ, Muench H. A simple method of estimating fifty per cent endpoints. *Am J Epidemiol*. 1938;27(3):493–7.
- Morris SK, Parkin P, Science M, Subbarao P, Yau Y, O'Riordan S, et al. A retrospective cross-sectional study of risk factors and clinical spectrum of children admitted to hospital with pandemic H1N1 influenza as compared to influenza A. *BMJ Open*. 2012;2(2):e000310.
- Ravanetti L, Dijkhuis A, Dekker T, Sabogal Pineros YS, Ravi A, Dierdorp BS, et al. IL-33 drives influenza-induced asthma exacerbations by halting innate and adaptive antiviral immunity. *J Allergy Clin Immunol*. 2019;143(4):1355–70.
- Irvin CG, Bates JH. Physiologic dysfunction of the asthmatic lung: what's going on down there, anyway? *Proc Am Thorac Soc*. 2009;6(3):306–11.
- Caminati M, Pham DL, Bagnasco D, Canonica GW. Type 2 immunity in asthma. *World Allergy Organ J*. 2018;11(1):13.
- Zhang H, Liu S, Li Y, Li J, Ni C, Yang M, et al. Dysfunction of S100A4(+) effector memory CD8(+) T cells aggravates asthma. *Eur J Immunol*. 2022;52(6):978–93.
- Furuya Y, Roberts S, Hurteau GJ, Sanfilippo AM, Racine R, Metzger DW. Asthma increases susceptibility to heterologous but not homologous secondary influenza. *J Virol*. 2014;88(16):9166–81.
- Jian YR, Chang SY, Lin PY, Yang YH, Chuang YH. Inactivated influenza virus vaccine is efficient and reduces IL-4 and IL-6 in allergic asthma mice. *Influenza Other Resp*. 2013;7(6):1210–7.
- Roy S, Williams CM, Furuya Y. Detrimental impact of allergic airway disease on live attenuated influenza vaccine. *Health Sci Rep*. 2021;4(3):e272.
- Chen J, Wang J, Zhang J, Ly H. Advances in development and application of influenza vaccines. *Front Immunol*. 2021;12:711997.
- Chen Y, Man-Tak Chu J, Liu JX, Duan YJ, Liang ZK, Zou X, et al. Double negative T cells promote surgery-induced neuroinflammation, microglial engulfment and cognitive dysfunction via the IL-17/CEBPbeta/C3 pathway in adult mice. *Brain Behav Immun*. 2024;123:965–81.
- Szabo E, Farago A, Bodor G, Gemes N, Puskas LG, Kovacs L, Szebeni GJ. Identification of immune subsets with distinct lectin binding signatures using multi-parameter flow cytometry: correlations with disease activity in systemic lupus erythematosus. *Front Immunol*. 2024;15:1380481.
- Lei H, Tian M, Zhang X, Liu X, Wang B, Wu R, Lv Y. Expansion of Double-Negative T Cells in Patients before Liver Transplantation Correlates with Post-Transplant Infections. *J Clin Med*. 2022;11(12).
- Passos LSA, Koh CC, Magalhaes LMD, Nunes M, Gollob KJ, Dutra WO. Distinct CD4(-)CD8(-) (double-negative) memory T-cell subpopulations

- are associated with indeterminate and cardiac clinical forms of chagas disease. *Front Immunol.* 2021;12:761795.
38. Neyt K, GeurtsvanKessel CH, Lambrecht BN. Double-negative T resident memory cells of the lung react to influenza virus infection via CD11c(hi) dendritic cells. *Mucosal Immunol.* 2016;9(4):999–1014.
 39. Park HJ, Lee SW, Park SH, Van Kaer L, Hong S. Selective expansion of double-negative iNKT cells inhibits the development of atopic dermatitis in Valpha14 TCR transgenic NC/Nga mice by increasing memory-type CD8(+) T and regulatory CD4(+) T cells. *J Investig Dermatol.* 2021;141(6):1512–21.
 40. Ferraz R, Cunha CF, Pimentel MIF, Lyra MR, Pereira-Da-Silva T, Schubach AO, et al. CD3(+)/CD4(neg)/CD8(neg) (double negative) T lymphocytes and NKT cells as the main cytotoxic-related-CD107a(+) cells in lesions of cutaneous leishmaniasis caused by *Leishmania (Viannia) braziliensis*. *Parasit Vectors.* 2017;10(1):219.
 41. Jalili Shahri J, Saeed Modaghegheh MH, Tanzadehpanah H, Ebrahimnejad M, Mahaki H. TH1/TH2 cytokine profile and their relationship with hematological parameters in patients with acute limb ischemia. *Rep Biochem Mol Biol.* 2024;13(1):31–9.
 42. Park SH, Jeon YH, Park YJ, Kim KY, Kim JS, Lee JB. Guaijaverin and epigallocatechin gallate complex modulate Th1 and Th2 cytokine-mediated allergic responses through STAT1/T-bet and STAT6/GATA3 pathways. *J Med Food.* 2024;27(9):844–56.
 43. Roth E, Pircher H. IFN-gamma promotes Fas ligand- and perforin-mediated liver cell destruction by cytotoxic CD8 T cells. *J Immunol.* 2004;172(3):1588–94.
 44. Xu A, Li Z, Ding Y, Wang X, Yang Y, Du L, et al. Electroacupuncture suppresses NK cell infiltration and activation in the ischemic mouse brain through STAT3 inhibition. *Brain Res Bull.* 2024;219:111128.
 45. Brigl M, Bry L, Kent SC, Gumperz JE, Brenner MB. Mechanism of CD1d-restricted natural killer T cell activation during microbial infection. *Nat Immunol.* 2003;4(12):1230–7.
 46. Lebrusant-Fernandez M, Ap Rees T, Jimeno R, Angelis N, Ng JC, Fraternali F, et al. IFN-gamma-dependent regulation of intestinal epithelial homeostasis by NKT cells. *Cell Rep.* 2024;43(12):114948.
 47. Montaldo E, Del Zotto G, Della Chiesa M, Mingari MC, Moretta A, De Maria A, Moretta L. Human NK cell receptors/markers: a tool to analyze NK cell development, subsets and function. *Cytometry A.* 2013;83(8):702–13.
 48. Kashyap MP, Mishra B, Sinha R, Jin L, Gou Y, Kumar N, et al. CD2 expressing innate lymphoid and T cells are critical effectors of immunopathogenesis in hidradenitis suppurativa. *Proc Natl Acad Sci USA.* 2024;121(48):e2409274121.
 49. El-Badawy O, Abbas AM, Radwan E, Makboul R, Khamis AA, Ali M, et al. Cross-talk between mucosal-associated invariant T, natural killer, and natural killer T cell populations is implicated in the pathogenesis of placenta accreta spectrum. *Inflammation.* 2023;46(4):1192–208.
 50. Han H, Lu Y, Xu S, Zhang W, Lin W, Zhan J, et al. Overcoming GABA-induced Treg suppression of immunity by ABAT to augment CD8+T cell anti-tumor immune response in liver cancer. *Int Arch Allergy Immunol.* 2024:1–16.
 51. Stiff PJ, Kertowidjojo E, Potkul RK, Banerjee S, Mehrotra S, Small W Jr, et al. Cabozantinib inhibits tumor growth in mice with ovarian cancer. *Am J Cancer Res.* 2024;14(10):4788–802.
 52. Phair IR, Sumoreeah MC, Scott N, Spinelli L, Arthur JSC. IL-33 induces granzyme C expression in murine mast cells via an MSK1/2-CREB-dependent pathway. *Biosci Rep.* 2022;42(12).
 53. An S, Jeon YJ, Jo A, Lim HJ, Han YE, Cho SW, et al. Initial influenza virus replication can be limited in allergic asthma through rapid induction of type III interferons in respiratory epithelium. *Front Immunol.* 2018;9:986.
 54. Chang LA, Choi A, Rathnasinghe R, Warang P, Nouredine M, Jangra S, et al. Influenza breakthrough infection in vaccinated mice is characterized by non-pathological lung eosinophilia. *Front Immunol.* 2023;14:1217181.
 55. Choi A, Ibanez LI, Strohmeier S, Krammer F, Garcia-Sastre A, Schotsaert M. Non-sterilizing, infection-permissive vaccination with inactivated influenza virus vaccine reshapes subsequent virus infection-induced protective heterosubtypic immunity from cellular to humoral cross-reactive immune responses. *Front Immunol.* 2020;11:1166.
 56. van den Toorn LM, Overbeek SE, de Jongste JC, Leman K, Hoogsteden HC, Prins JB. Airway inflammation is present during clinical remission of atopic asthma. *Am J Respir Crit Care Med.* 2001;164(11):2107–13.
 57. Kim MS, Cho KA, Cho YJ, Woo SY. Effects of interleukin-9 blockade on chronic airway inflammation in murine asthma models. *Allergy Asthma Immunol Res.* 2013;5(4):197–206.
 58. Samarasinghe AE, Melo RC, Duan S, LeMessurier KS, Liedmann S, Surman SL, et al. Eosinophils promote antiviral immunity in mice infected with influenza A virus. *J Immunol.* 2017;198(8):3214–26.
 59. Zhou J, Liu J, Wang B, Li N, Liu J, Han Y, Cao X. Eosinophils promote CD8(+) T cell memory generation to potentiate anti-bacterial immunity. *Signal Transduct Target Ther.* 2024;9(1):43.
 60. Phipps S, Lam CE, Mahalingam S, Newhouse M, Ramirez R, Rosenberg HF, et al. Eosinophils contribute to innate antiviral immunity and promote clearance of respiratory syncytial virus. *Blood.* 2007;110(5):1578–86.
 61. Bjerregaard A, Laing IA, Backer V, Fally M, Khoo SK, Chidlow G, et al. Clinical characteristics of eosinophilic asthma exacerbations. *Respirology.* 2017;22(2):295–300.
 62. Fukuda Y, Hayashi H, Sagara H. COVID-19-induced eosinophilic lower airway inflammation in those with multiple COVID-19 vaccinations. *Cureus.* 2023;15(5):e38368.
 63. Antuna VL, Puchades F, Tapial JM, Ribelles JC, Sanz F, Tamarit JJ. Eosinophilic fasciitis following SARS-CoV-2 vaccination. *JAAD Case Rep.* 2023;36:11–4.
 64. Hojberg Y, Abdeljaber M, Prahlow JA. Generalized eosinophilia following moderna COVID-19 vaccine administration: a case report. *Acad Forensic Pathol.* 2023;13(1):9–15.

Publisher's Note

Springer Nature remains neutral with regard to jurisdictional claims in published maps and institutional affiliations.